*Journal of The Electrochemical Society*, **150** (9) C631-C634 (2003)
0013-4651/2003/150(9)/C631/4/$7.00 © The Electrochemical Society, Inc.

# Selective Growth of Carbon Nanotubes on Prepatterned Amorphous Silicon Thin Films by Electroless Plating Ni

**C. W. Chao,[*,z] YewChung Sermon Wu, Gau-Ren Hu,[*] and Ming-Shian Feng**

*Department of Materials Science and Engineering, National Chiao Tung University, Hsinchu 300, Taiwan, China*

Selective growth of carbon nanotubes (CNTs) synthesized at low temperature by electroless plating Ni was proposed for the first time in this study. After electroless plating, Ni nanoparticles were selectively deposited on the prepatterned amorphous silicon (a-Si) thin films. After plasma-enhanced chemical vapor deposition, well-aligned CNTs were observed only on the Ni-coated a-Si islands. The diameter, density, and the field emission of CNTs could be controlled easily by the Ni plating time. The achievement of controlling the site density and growth area is significant for applications of carbon nanotubes as field emission devices, nanoelectrode arrays, etc.
© 2003 The Electrochemical Society. [DOI: 10.1149/1.1596953] All rights reserved.

Manuscript submitted September 23, 2002; revised manuscript received March 12, 2003. Available electronically July 30, 2003.

Carbon nanotubes (CNTs) have attracted extensive attention due to their unique physical properties and applications.[1-5] One of the most attractive applications of CNTs is the electron emitter for field emission displays because CNTs have a low field emission voltage and a large current density.[6-8] For field emission displays, the substrates are usually made of glass substrate because of its low price and good vacuum sealing. Therefore the growth temperature of CNTs for field emission displays must be lower than glass strain temperature (600°C).

Intensive studies have been done to lower the synthesis temperature of CNTs.[9-12] Metal catalyst is one of these efforts, in which Ni, Fe, and Co are used either separately or together as composite catalysts.[6-15] When CNTs were synthesized with low temperature, the size of metal catalysts needs as small as possible because the size of metal catalysts must be smaller than the diffusion length of carbon,[16] which increased with the temperature.

The diameter and the site density of CNTs can be controlled by changing the particle size and the site density of catalysts.[15,17] The density of catalysts can be controlled by lithography,[18,19] micro-contact printing,[20] shadow mask,[4] etc. However, all these methods either require expensive equipment and intensive labor or cannot control the site density in large area.[15] In order to control the site density of the catalysts, Tu *et al.* used the pulse-current electrochemical deposition technique to prepare Ni nanoparticles.[15] The experiment was carried out on a two-electrode system. The working electrode was prepared by sputtering a layer of Cr on a silicon wafer to get a conductive surface. The nucleation site density of the Ni nanoparticles was controlled by changing the magnitude and duration of the pulse current. After plasma enhanced (PE) hot filament chemical vapor deposition (CVD), the site density of the aligned CNTs varied from $10^5$ to $10^8$ $cm^{-2}$.

In addition to the site density of CNTs, the selective growth of CNTs is another important issue for the application of field emission displays. In a previous study, Chen *et al.*[14] proposed a new field emission device composed of carbon nanotubes and a thin film transistor (TFT), in which iron film was selectively deposited on the drain area of poly-Si TFT which was followed by synthesis of the CNTs on the drain area. They found that the emission stability has been significantly improved.

In this study, a similar electrochemical deposition technique as described in Ref. 21 was used. An electroless plating Ni method was introduced to control the growth of Ni nanoparticles. During the plating process, Ni nanopartilces were deposited by a redox reaction. Since there was no external current and voltage involved, no conductive electrode layer was required. To control the deposition of the Ni nanoparticles, a-Si films were patterned by photolithography before plating. After the PECVD process, CNTs were found to grow selectively on the a-Si islands.

* Electrochemical Society Student Member.
z E-mail: jeffchao.mse88g@nctu.edu.tw

## Experimental

The substrates used in this study were 1 × 1 cm silicon (100) chips with 500 nm thick $SiO_2$ films, which simulated the glass substrate. Amorphous silicon (a-Si) films with a thickness of 100 nm were then deposited by a low-pressure CVD (LPCVD) system at 550°C. Amorphous Si islands were defined by photolithography and etched by reactive ion etching (RIE) method. The samples were cleaned with a solution of $H_2SO_4$ and $H_2O_2$. After being dipped into the diluted HF solution to remove the native oxide on the samples, the samples were dipped into the plating solution for 60, 90, or 120 s to coat Ni nanoparticles. The composition of plating solution was $NiCl_2 \cdot 6H_2O$ 30 g $L^{-1}$, $NH_4Cl$ 50 g $L^{-1}$, $NaH_2PO_3$ $H_2O$ 10 g $L^{-1}$, and $C_6H_5Na_3O_7$ $H_2O$ 84 g $L^{-1}$.[21] The plating temperature was kept at 80°C and the PH value of the plating solution was 8.0.

After electroless plating, the substrates with Ni nanoparticles were loaded into a PECVD chamber, where CNT growth was performed. Before the growth of CNTs, $H_2$ gas was introduced into the chamber to activate the surface of Ni nanoparticles for 10 min The pressure of reaction was 20 Torr and the flow rate of $H_2$ was 80 standard cubic centimeter per minute (sccm). The microwave plasma input power was 1000 W and the substrate temperature was 580°C. To grow the CNTs, a mixture of methane and hydrogen gases was then admitted to the chamber. The flow rates of methane and hydrogen were 4 and 80 sccm, and the negative bias of substrate was −100 V.

Field emission measurements were carried out on these samples using the apparatus shown in Fig. 1. The anode electrode was placed 100 μm away from the substrate. The size of measured field emitting area was 5 $mm^2$.

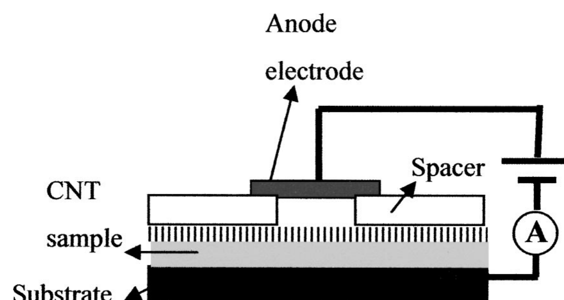


**Figure 1.** Schematic diagram of the field emission measurement apparatus.

Downloaded on 2014-04-27 to IP 140.113.38.11 address. Redistribution subject to ECS terms of use (see ecsdl.org/site/terms_use) unless CC License in place (see abstract).

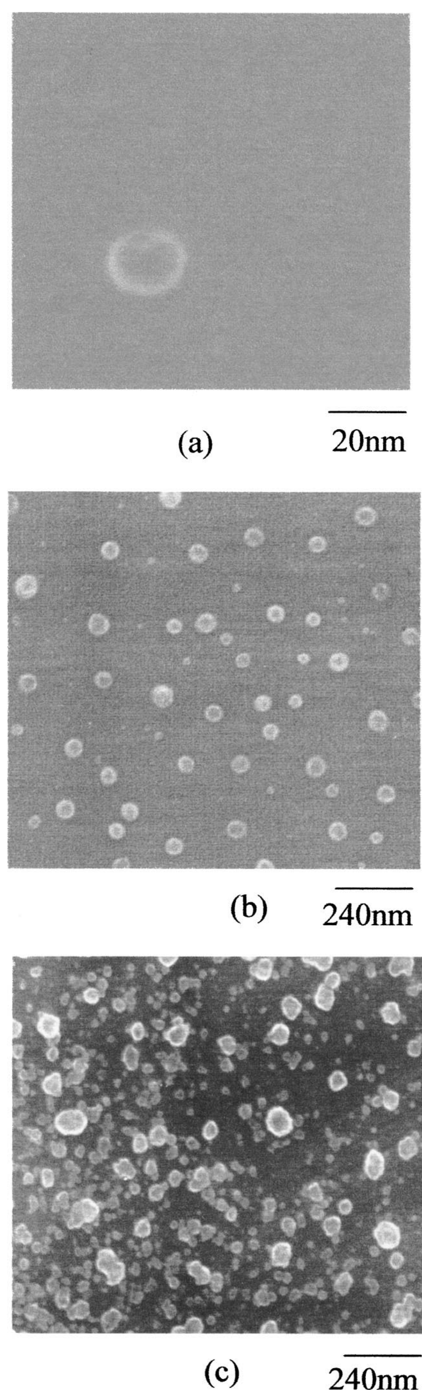


**Figure 2.** SEM images of Ni nanoparticles on the a-Si patterns after electroless Ni plating for (a) 60 s, (b) 90 s, and (c) 120 s.

**Table I. Effects of Ni plating time on the site density and diameter of Ni nanoparticles, and the diameter of CNTs.**

| Ni plating time (s) | Density of Ni nanoparticles (particle/cm$^2$) | Diameter of Ni nanoparticles (nm) | Diameter of CNTs (nm) |
|---|---|---|---|
| 60 | $7 \times 10^7$ | 20-30 | 20-45 |
| 90 | $2 \times 10^9$ | 40-80 | 60-80 |
| 120 | $1 \times 10^{10}$ | 30-150 | 75-200 |

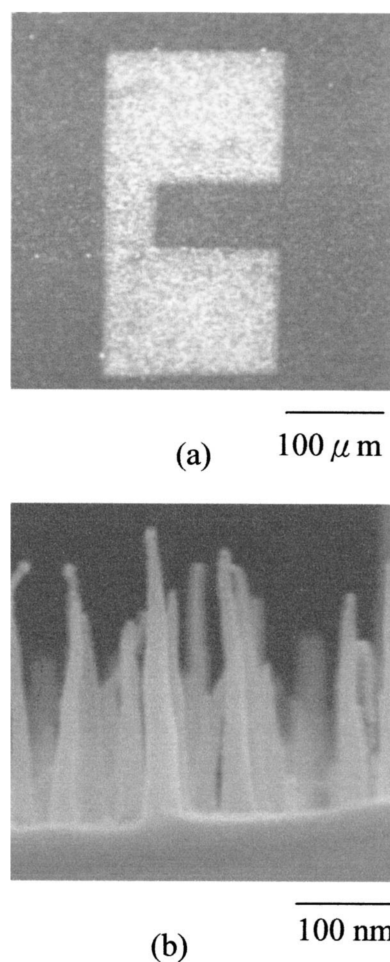


**Figure 3.** (a) SEM image of CNTs selectively synthesized on the a-Si patterns, and (b) high resolution SEM image of these vertical aligned CNTs.

## Results and Discussion

The scanning electron microscope (SEM) images of Ni nanoparticles with various lengths of plating time are shown in Fig. 2. Regardless of the plating time (60-120 s), no Ni cluster was found on the oxide area. The Ni nanoparticles were only selectively deposited on the a-Si islands. When the plating time was 60 s, the typical diameter of Ni nanoparticles was about 20 nm and the density of Ni nanoparticles was $7 \times 10^7/\text{cm}^2$. As shown in Fig. 2 and Table I, the density and the size of Ni nanoparticles increased monolithically with the plating time, as expected. When the plating time increased to 120 s, the diameter of Ni nanoparticles reached 150 nm and the density reached $1 \times 10^{10}/\text{cm}^2$. Figure 3a shows the typical SEM images of samples after the growth of CNTs. The light features seen in the micrographs correspond to CNTs grown on the top of a-Si islands. CNTs were only selectively synthesized on the Ni-coated a-Si islands. No CNT was found on the oxide surface. The nature of the well-aligned CNTs was verified using SEM as shown in Fig. 3b. The advantages of Ni catalysts prepared by electroless plating are illustrated in Fig. 4. The Ni catalysts were only deposited on the a-Si island but not on the oxide surface. Therefore, during low temperature CNT synthesis, CNTs could be selectively synthesized on the a-Si pattern without using the lithograph process.

When the plating time was 60 s, the diameter of the bottom of CNTs was 45 nm, while the diameter of the top of CNTs was only 20 nm. These carbon nanotips were formed because CNTs were anisotropically etched by hydrogen plasma.[22-24] It is believed that during the growth of CNTs, the active carbon species in the plasma are accelerated to the substrate by the negative bias to form the

Downloaded on 2014-04-27 to IP 140.113.38.11 address. Redistribution subject to ECS terms of use (see ecsdl.org/site/terms_use) unless CC License in place (see abstract).

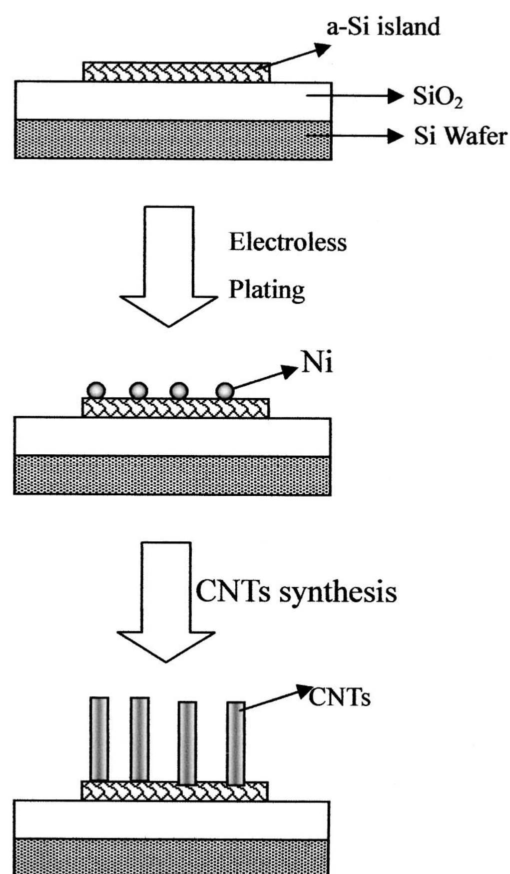


**Figure 4.** The electroless plating processes for CNTs synthesis.

CNTs. Meanwhile, the accelerated active hydrogen radicals etch the top of CNTs and form the carbon nanotips.[23] Fortunately, the formation of these nanotips could enhance the field emission of CNTs.[24]

It was also found that the density of CNTs increased with the Ni plating time, as shown in Fig. 5. This is due to that CNTs were induced by Ni particles. As shown in Fig. 1 and Table I, the density of Ni particles increased with the plating time; therefore, the density of CNTs increased. Figure 5 and Table I also indicate that the diameter of CNTs increased with the plating time. In other words, the larger the Ni nanoparticles, the larger the CNTs. This result is consistent with the conclusion drawn by Ref. 15 and 17, during their CNT growth studies. They found that larger catalyst particles produced larger CNTs. As shown in Fig. 4, the diameters of the top of CNTs were also found to be sharpened by the anisotropically hydrogen plasma etching, regardless of the Ni plating time. Fortunately, this reduction of the CNTs diameter could enhance the field emission of CNTs.

The field emission current of CNTs versus applied electric field is shown in Fig. 6. The threshold field, which was defined as the current densities reached 1 $\mu$A cm$^{-2}$, was significantly affected by the Ni plating time. When the Ni plating time was 60 s, the threshold field was 4.5 V/$\mu$m where the current started to increase exponentially with electric field. When the plating time increased to 90 s, the threshold field decreased to 3.5 V/$\mu$m. With further increase of the plating time to 120 s, the threshold field, however, did not decrease but increased to 4.0 V/$\mu$m.

Two factors can affect the threshold field (field emission current): the radius (diameter) of CNTs and density of CNTs. The effect of the radius on the field emission current can be deduced from the Fowler-Nordheim model.[25,26] In this model, the dependence of the emitted current $I$ on the local electric field $F$ and the work function $\Phi$ is given by

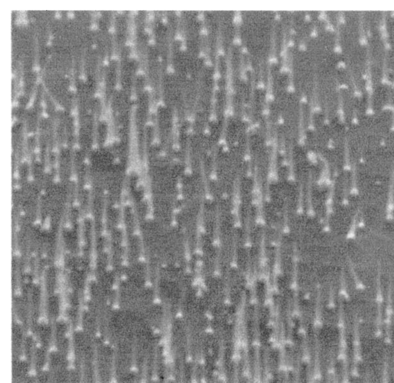


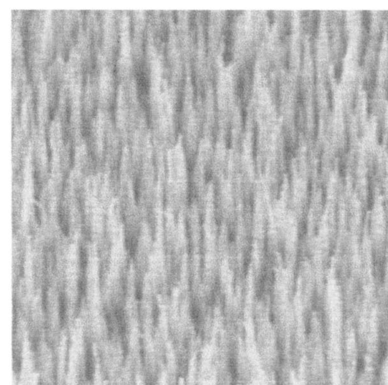


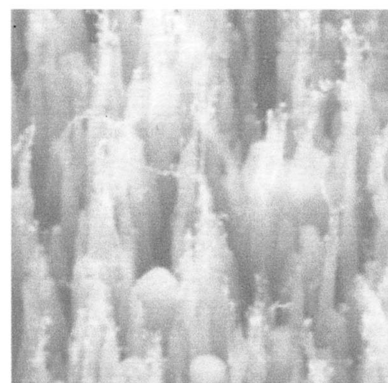


**Figure 5.** SEM images of CNTs on the a-Si patterns with electroless Ni plating for (a) 60 s, (b) 90 s, and (c) 120 s.

$$I \alpha (F^2/\Phi)\exp(-B\Phi^{3/2}/F) \quad [1]$$

where $B = 6.83 \times 10^9$ (V eV$^{-3/2}$ m$^{-1}$). The local electric field $F$ is not simply $V/d_o$, which is the macroscopic electric field obtained by applying a voltage $V$ between two planar and parallel electrodes separated by a distance $d_o$. The local field is given by

$$F = \beta V/d_o \quad [2]$$

where $\beta$ is determined by the shape of the emitter, and especially by its radius of curvature at the tip, $r_o$. The basic approximation of $\beta$ is

Downloaded on 2014-04-27 to IP 140.113.38.11 address. Redistribution subject to ECS terms of use (see ecsdl.org/site/terms_use) unless CC License in place (see abstract).

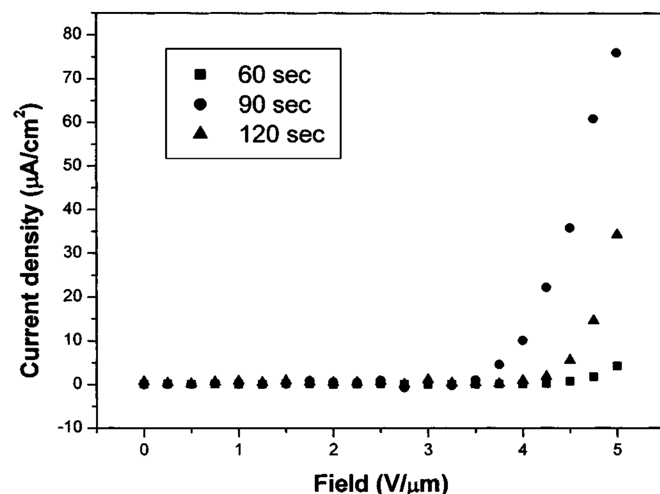


**Figure 6.** Emission current *vs.* applied electric field curves.

$$\beta \simeq d/(kr_o) \quad [3]$$

where $k$ is a constant. Combining Eq. 1, 2, and 3, it is clear that both the local field $F$ and emitted current $I$ increased with decreasing radius of curvature. In other words, the threshold field increases with the diameters of CNTs.

Besides the diameter of the CNTs, the density of the CNTs also affects the threshold field. When the density of the CNTs increased, the distance between CNTs became shorter, which degraded the field emission of CNTs due to the screening effect.[27,28]

In this study, since the diameter increased with the Ni plating time, the threshold field of each CNT increased with the plating time. However, the density of CNTs increased significantly from $7 \times 10^7$ to $1 \times 10^{10}$/cm$^2$; therefore, the total emission current of CNTs still increased. In other words, the threshold field of CNTs decreased when the plating time increased from 60 to 90 s. With further increase of the plating time to 120 s, the diameter and density of CNTs became too large. The threshold field of each CNT increased and the short distance between CNTs degraded the field emission of CNTs. Therefore, the threshold field increased to 4.0 V/μm.

## Conclusions

Selective growth of vertical aligned CNTs on the prepatterned amorphous silicon islands by electroless plating Ni has been observed for the first time in this study. The synthesis temperature of CNTs was as low as 580°C due to the Ni cluster catalyst. The diameter and density of Ni nanoparticles were found to increase with the Ni plating time. Since CNTs were induced by Ni nanoparticles, the density and diameter of CNTs could be easily controlled by the Ni plating time. Therefore, the field emission properties of CNTs could also be controlled by plating time. Using this selective growth of vertical aligned CNTs, this simple process may be adequate for integration of CNTs into TFT on glass substrates, nanoelectrode arrays and other devices.

## Acknowledgments

This research was supported in part by the National Science Council (NSC) of the Republic of China under grant NSC 91-2215-E009-046. Technical supports from the National Nano Device Laboratory of NSC and Semiconductor Research Center of National Chiao Tung University are also acknowledged.

*National Chiao Tung University assisted in meeting the publication costs of this article.*

## References

1. R. Saito, M. Fujita, G. Dresselhaus, and M. S. Dresselhaus, *Appl. Phys. Lett.,* **60**, 2204 (1992).
2. G. Che, B. B. Lakshmi, E. R. Fisher, and C. R. Martin, *Nature (London),* **398**, 346 (1998).
3. A. C. Dillon, K. M. Jonse, T. A. Bekkedahl, C. H. Kiang, D. S. Bethune, and M. J. Heben, *Nature (London),* **386**, 377 (1997).
4. S. Fan, M. G. Chapline, N. R. Franklin, T. W. Tombler, A. M. Cassell, and H. Dai, *Science,* **283**, 512 (1999).
5. C. Zhou, J. Kong, and H. Dai, *Appl. Phys. Lett.,* **76**, 1597 (2000).
6. W. A. deHeer, A. Chatelain, and D. Ugarte, *Science,* **270**, 1179 (1995).
7. W. Zhu, C. Bower, O. Zhou, G. Kochanski, and S. Jin, *Appl. Phys. Lett.,* **75**, 873 (1999).
8. K. A. Dean and B. R. Chalamala, *Appl. Phys. Lett.,* **75**, 3017 (1999).
9. Z. F. Ren, Z. P. Huang, J. W. Xu, J. H. Wang, P. Bush, M. P. Siegal, and P. N. Provncio, *Science,* **282**, 1105 (1998).
10. J. H. Han, H. J. Kim, M. H. Yang, C. W. Yang, J. B. Yoo, C. Y. Park, Y. H. Song, and K. S. Nam, *Mater. Sci. Rep.,* **16**, 65 (2001).
11. G. W. Ho, A. T. S. Wee, J. Lin, and W. C. Tjiu, *Thin Solid Films,* **388**, 73 (2001).
12. C. Klinke, J. M. Bonard, and K. Kern, *Surf. Sci.,* **492**, 191 (2001).
13. J. Kim and K. No, *J. Appl. Phys.,* **90**, 2591 (2001).
14. H. C. Cheng, W. K. Hong, F. G. Tarntair, K. J. Chen, J. B. Lin, K. H. Chen, and L. C. Chen, *Electrochem. Solid-State Lett.,* **4**, H5 (2001).
15. Y. Tu, Z. P. Hung, D. Z. Wang, J. G. Wen, and Z. F. Ren, *Appl. Phys. Lett.,* **80**, 4018 (2002).
16. Y. Y. Wei, G. Eres, V. I. Merkulov, and D. H. Lowndes, *Appl. Phys. Lett.,* **78**, 1394 (2001).
17. Z. P. Hung, D. Z. Wang, J. G. Wen, M. Sennett, H. Gilbson, and Z. F. Ren, *Appl. Phys. A: Mater. Sci. Process.,* **74**, 387 (2002).
18. Z. F. Ren, Z. P. Hung, D. Z. Wang, J. G. Wen, J. W. Xu, J. H. Wang, L. E. Calvet, J. Chen, J. F. Klemic, and M. A. Reed, *Appl. Phys. Lett.,* **75**, 1086 (1999).
19. H. Murakami, M. Hirakawa, C. Tanaka, and H. Yamakawa, *Appl. Phys. Lett.,* **76**, 1776 (2000).
20. L. Nilsson, O. Groening, C. Emmenegger, O. Kuettel, E. Schaller, L. Schlapbach, H. Kind, J. M. Bonard, and K. Kern, *Appl. Phys. Lett.,* **76**, 2071 (2000).
21. A. Brenmer, *Met. Finish.,* **11**, 53 (1954).
22. S. H. Tsai, C. W. Chao, C. L. Lee, and H. C. Shih, *Appl. Phys. Lett.,* **74**, 3462 (1999).
23. C. L. Tsai, C. F. Chen, and L. K. Wu, *Appl. Phys. Lett.,* **81**, 721 (2002).
24. X. D. Bai, C. Y. Zhi, S. Liu, E. G. Wang, and Z. L. Wang, *Solid State Commun.,* **125**, 185 (2003).
25. J. M. Bonard, M. Croci, I. Arfaoui, O. Noury, D. Sarangi, and A. Châtelain, *Diamond Relat. Mater.,* **11**, 763 (2002).
26. J. M. Bonard, M. Croci, C. Klinke, R. Kurt, O. Noury, and N. Weiss, *Carbon,* **40**, 1715 (2002).
27. R. Kurt, J. M. Bonard, and A. Karimi, *Thin Solid Films,* **398**, 193 (2001).
28. K. B. K. Teo, M. Chhowalla, G. A. J. Amaratunga, W. I. Milne, G. Pirio, P. Legagneux, F. Wyczisk, D. Pribat, and D. G. Hasko, *Appl. Phys. Lett.,* **80**, 2011 (2002).

Downloaded on 2014-04-27 to IP 140.113.38.11 address. Redistribution subject to ECS terms of use (see ecsdl.org/site/terms_use) unless CC License in place (see abstract).